REVIEW

Feedstock choice, pyrolysis temperature and type influence biochar characteristics: a comprehensive meta-data analysis review

James A. Ippolito[1] · Liqiang Cui[1,2] · Claudia Kammann[3] · Nicole Wrage-Mönnig[4] · Jose M. Estavillo[5] · Teresa Fuertes-Mendizabal[5] · Maria Luz Cayuela[6] · Gilbert Sigua[7] · Jeff Novak[7] · Kurt Spokas[8] · Nils Borchard[9]

Abstract

Various studies have established that feedstock choice, pyrolysis temperature, and pyrolysis type influence final biochar physicochemical characteristics. However, overarching analyses of pre-biochar creation choices and correlations to biochar characteristics are severely lacking. Thus, the objective of this work was to help researchers, biochar-stakeholders, and practitioners make more well-informed choices in terms of how these three major parameters influence the final biochar product. Utilizing approximately 5400 peer-reviewed journal articles and over 50,800 individual data points, herein we elucidate the selections that influence final biochar physical and chemical properties, total nutrient content, and perhaps more importantly tools one can use to predict biochar's nutrient availability. Based on the large dataset collected, it appears that pyrolysis type (fast or slow) plays a minor role in biochar physico- (inorganic) chemical characteristics; few differences were evident between production styles. Pyrolysis temperature, however, affects biochar's longevity, with pyrolysis temperatures > 500 °C generally leading to longer-term (i.e., > 1000 years) half-lives. Greater pyrolysis temperatures also led to biochars containing greater overall C and specific surface area (SSA), which could promote soil physico-chemical improvements. However, based on the collected data, it appears that feedstock selection has the largest influence on biochar properties. Specific surface area is greatest in wood-based biochars, which in combination with pyrolysis temperature could likely promote greater changes in soil physical characteristics over other feedstock-based biochars. Crop- and other grass-based biochars appear to have cation exchange capacities greater than other biochars, which in combination with pyrolysis temperature could potentially lead to longer-term changes in soil nutrient retention. The collected data also suggest that one can reasonably predict the availability of various biochar nutrients (e.g., N, P, K, Ca, Mg, Fe, and Cu) based on feedstock choice and total nutrient content. Results can be used to create designer biochars to help solve environmental issues and supply a variety of plant-available nutrients for crop growth.

Keywords Biochar · Total elemental analysis · Plant-available elemental analysis · Physico-chemical characteristics · Meta-analysis

1 Introduction

Biochars are carbon (C) rich materials typically produced via biomass pyrolysis at relatively low temperatures (300–700 °C) under limited oxygen conditions (Lehmann and Joseph 2009). Biomass, the feedstock for biochar

✉ Nils Borchard
nils.borchard@luke.fi

Extended author information available on the last page of the article

creation, is typically derived from agricultural and forestry waste products, municipal waste, green and food waste. The creation of biochar from these products places C into a recalcitrant form which could last hundreds to over thousands of years (Spokas 2010; Kuzyakov et al. 2014; Wang et al. 2016), suggesting that biochar could aid in climate change mitigation (Tripathi et al. 2016) as one of the few negative greenhouse gas emission technologies with sustainable development co-benefits (Smith et al. 2019).

Over shorter time scales (e.g., one to several years), biochars have been proven to improve environmental quality by sorbing heavy metals and organic contaminants (e.g., Sigua et al. 2019; Cui et al. 2019; Novak et al. 2019a), positively

affect soil water relations (e.g., Lentz et al. 2019; Kammann et al. 2011), reduce greenhouse gas emissions (e.g., Fuertes-Mendizábal et al. 2019; Borchard et al. 2018; Jeffery et al. 2016), and improve crop growth (e.g., Laird et al. 2017; Novak et al. 2016; Liu et al. 2013). Although creation of biochars for the above purposes may seem simply based on feedstock selection, biochar production for environmental improvements is complex. Feedstock selection, pyrolysis temperatures, and pyrolysis types can all greatly influence the final biochar product (Cao et al. 2017; Cha et al. 2016). Thus, increasing the understanding of the interaction between feedstock, pyrolysis temperature, and production technique (i.e., either fast or slow pyrolysis) would help biochar stakeholders make more well-informed choices for its use.

In terms of feedstock, understanding how initial feedstock properties influence final biochar characteristics is important. Feedstocks have been shown to play a major role in creating biochars with distinctly different chemical properties (Funke and Ziegler 2010; Novak et al. 2019b). In relative terms, wood-based biochars contain more C and lower plant-available nutrients, manure-based biochars show opposite trends, and grass-based biochars typically fall somewhere in between woody and manure biochars (Ippolito et al. 2015). However, these properties may be altered by pyrolysis temperature and pyrolysis technique used for biochar creation.

Pyrolysis temperature and production technique play key roles in creating biochars with various chemical and structural properties. For example, nutrient availability changes drastically as pyrolysis temperature is increased (Clough et al. 2013; Nguyen et al. 2017). Specifically, with increasing pyrolysis temperature one typically observes increasing biochar C, P, K, Ca, ash content, pH, specific surface area (SSA), and decreasing N, H, and O content (e.g., Weber and Quicker 2018; Ippolito et al. 2015). These biochar characteristics are driven by forcing C into more condensed, recalcitrant forms, the creation of oxide/carbonate mineral phases (e.g., P, K, Ca) leading to greater ash content and higher pH, and the loss of N, H, and O via volatilization. Volatilization losses further concentrate other remaining elements (Kim et al. 2012; Kinney et al. 2012). When choosing pyrolysis type, in general slow pyrolysis tends to produce biochars with greater N, S, available P, Ca, Mg, surface area, and cation exchange capacity (CEC) as compared to fast pyrolysis.

The above aspects of biochar creation have led individual researchers to pay attention to biochar end-product properties. Current literature contains an untapped wealth of information regarding feedstock, pyrolysis type and temperature choices. However, there is some uncertainty in the literature with a vague description of how biochar characteristics are influenced by feedstock choice, pyrolysis type, and temperature employed. Thus, we chose to provide in this review a clearer picture by synthesizing existing literature to create

a true comprehensive review of biochar properties based on feedstock choice, pyrolysis temperature, and pyrolysis type. Presenting this type of data is paramount for improving our understanding of the factors used to create biochar and characteristics within the final product. Establishing these comparisons should aid biochar practitioners and stakeholders in making well-informed decisions for biochar use as amendments in soils and for environmental mitigation purposes in mine spoils or metal contaminated soils. The objective of this work was focused on comprehensively reviewing how different feedstocks, pyrolysis temperatures, and production techniques affect biochar physicochemical properties, total and available nutrient content, other characteristics, and what these properties indicate when biochar is used for agricultural benefits.

2 Materials and methods

Data were compiled from literature that compared biochar macro- and micro-nutrient concentrations, pH, SSA, electrical conductivity (EC), cation and anion exchange capacity (CEC and AES, respectively), calcium carbonate equivalent (CCE), total pore volume (PV), average particle size (APS), and ash content under different biochar production temperatures and types. The literature examined was published between January 2009 through December 2016, searching electronic databases including Web of Science™ and Scopus™ for the keyword "biochar". Overall, 5394 publications presented reliable and valid physicochemical biochar properties which were fed into a database obtaining 50,851 individual observations (see Supporting Table 1 for references cited). We chose not to collect data from 2016 onwards because of the overwhelming points already collected from between 2009 and 2016.

Data from the selected peer-reviewed literature should provide the reader with overarching changes in biochar physicochemical characteristics, and thus where appropriate, specific inferences were made based on logical comparisons between biochar properties. The data are presented by feedstock choice, pyrolysis temperature, and pyrolysis type (i.e., either fast or slow pyrolysis). The data are further separated into nutrient availability based on feedstock choice, in order to provide biochar producers with guidance for preparing biochars to meet plant nutrient needs.

2.1 Feedstock choice

Wood feedstock data were derived from literature reporting chipped, shaved, bark, peeled, and other similar wood-based biochar products. All wood data were initially combined into one category because it has been previously shown that, in general, hardwood and softwood biochars have similar

characteristics (Ippolito et al. 2015). However, this concept was revisited in the current manuscript due to the larger dataset involved as compared to Ippolito et al. (2015); wood feedstock data were further separated into either hardwood- (including bamboo) or softwood-derived biochars for specific nutrient availability analysis presented below.

Crop waste data included biochars made from a variety of agricultural crop residues, such as corn, wheat straw, rice straw and husk, potato, soybean, sugarcane and bagasse, cotton, grape, orange, peanut, and rape seed/straw. Based on the dataset collected, the major crop wastes utilized to produce biochars were corn, wheat straw, and rice straw/husk, and, therefore, this datum was further categorized for derivation of specific nutrient availability analyses presented below.

Other results from grasses were compiled from species that were typically, but not entirely, used for bioenergy, industrial production, or fodder. This dataset included grassy and leafy species such as Miscanthus (*Miscanthus spp.*), switchgrass (*Panicatum virgatum*), giant red (*Arundo spp.*), common reed (*Phragmites australis*), Typha (*Typha spp.*), water hyacinth (*Eichhornia crassipes*), and other minor grass species. Opposite of other feedstocks, this dataset was not further refined for nutrient availability analyses due to a lack of dataset robustness.

The manures/biosolids dataset included biochars made from papermill sludges, cattle and dairy manure, horse manure, swine manure, poultry manure and litter, and biosolids. Among all feedstocks, poultry manure, pig manure, cattle and dairy manure, and biosolids were the most common feedstocks employed to produce biochars. Thus, biochars made from these four feedstock choices were further separated for defining their specific nutrient availability as presented below.

2.2 Pyrolysis temperature and type

For ease of discussion, pyrolysis temperatures were grouped as follows: < 300, 300–399, 400–499, 500–599, 600–699, 700–799, and > 800 °C. A similar approach was utilized by Ippolito et al. (2015) when describing changes in biochar properties as affected by pyrolysis temperature. Pyrolysis type was simply separated into either fast or slow pyrolysis as indicated in the manuscripts evaluated.

2.3 Data interpretation

All individual data comparisons (e.g., total C, total O, total, H, etc.) between fast or slow pyrolysis were analyzed using a t test at $\alpha = 0.05$. All individual data comparisons between various feedstocks or all pyrolysis temperatures were analyzed using analysis of variance (ANOVA). The Shapiro–Wilk and Levene's tests were also used to analyze for assumptions of normality and equal variance,

respectively. In cases where assumptions were violated, data were transformed using either $\log_{10}$, natural log, or a square root function and re-analyzed for meeting assumptions of normality and equal variance. Tukey's Honestly Significant Difference pairwise comparisons were utilized to discern differences between various feedstocks or pyrolysis temperatures for individual (non-)transformed data at $\alpha = 0.05$. The non-transformed data means are presented below.

For more specific data interpretations, we utilized the entire dataset, or specific feedstock subsets, along with SigmaPlot 13.0 for graphical interpretations. Within SigmaPlot 13.0, we utilized regression fitting functions (linear, quadratic, exponential rise or decay, and exponential growth equations) that best fit (e.g., best R^2 values and greatest p values) the presented data. We avoided data interpretations that made no logical sense (e.g., sigmoidal equations, sinusoidal equations, etc.) yet may have had greater R^2 values than regression equations that made logical, interpretable sense. When necessary, Pearson's correlations were utilized to help drive discussion for biochar utilization from specific feedstock choices.

3 Results and discussion

3.1 Biochar physicochemical properties

3.1.1 Pyrolysis type

In terms of the general utility in choosing pyrolysis type, slow pyrolysis uses a slow temperature heating rate (0.01–2 °C s^{-1}) as compared to fast pyrolysis, and if adjusted properly can produce approximately equal ratios of solid (i.e., biochar), gas, and liquid products (Sohi et al. 2009). Fast pyrolysis uses higher heating rates (> 2 °C s^{-1}) and shorter residence times (< 2 s) during the thermal conversion process, which provides greater bio-oil yields (75%) but lower gas and biochar quantities (Qambrani et al. 2017).

The influence of pyrolysis type on final biochar physicochemical properties is presented in Table 1. Fast pyrolysis led to biochars containing greater SSA and lower APS as compared to slow pyrolysis, both parameters likely a function of the relatively small initial feedstock particle size utilized during fast pyrolysis in fluidized bed reactor (Asadullah et al. 2010). Slow pyrolysis led to biochars containing greater CCE and ash content as compared to fast pyrolysis. Increasing ash content and CCE are related, as acidic functional groups are reduced (Novak et al. 2009) and mineral hydroxide and carbonate phases are increased with increasing ash content (Knicker 2007).

Table 1 Basic biochar mean physicochemical properties (± standard error of the mean) based on pyrolysis type, feedstock source, and pyrolysis temperature, on a dry weight basis

	SSA (m² g⁻¹)	CEC (cmol kg⁻¹)	AEC (cmol kg⁻¹)	CCE (%)	PV (m³ t⁻¹)	APS (nm)	Ash (%)	pH	EC (dS m⁻¹)
Pyrolysis type									
Fast	183 ± 17.3a	44.9 ± 3.62	4.90 ± 3.45	6.10 ± 1.12b	2.04 ± 0.81	52.3 ± 40.2b	19.2 ± 0.62b	8.7 ± 0.1	4.43 ± 0.50
Slow	98.6 ± 3.53b	48.1 ± 3.12	5.33 ± 1.51	11.2 ± 0.98a	3.66 ± 1.27	1190 ± 565a	22.0 ± 0.51a	8.7 ± 0.0	5.85 ± 1.58
Feedstock source									
Wood based	184 ± 11.4a	23.9 ± 1.87b	5.65 ± 1.80	9.04 ± 1.17b	7.01 ± 3.07a	74.6 ± 44.4a	10.2 ± 0.43d	8.3 ± 0.1b	6.20 ± 2.85
Crop wastes	98.2 ± 5.45b	56.3 ± 3.92a	4.51 ± 1.96	6.12 ± 0.97b	2.05 ± 0.91b	2320 ± 1,150a	21.1 ± 0.54b	8.9 ± 0.1a	5.72 ± 0.67
Other grasses	63.4 ± 8.84b	63.3 ± 16.4a	2.05 ± 1.05	ND	3.36 ± 3.30a	268 ± 125a	18.0 ± 1.01c	8.9 ± 0.1a	5.20 ± 0.93
Manures/ Biosolids	52.2 ± 4.23c	66.1 ± 8.00a	7.77 ± 7.52	14.2 ± 1.56a	0.82 ± 0.30b	27.3 ± 12.5b	44.6 ± 0.97a	8.9 ± 0.1a	3.98 ± 0.41
Pyrolysis temp (°C)									
< 300	27.1 ± 5.45c	44.4 ± 6.43ab	ND	7.16 ± 0.81	0.06 ± 0.02ab	8.16 ± 1.57	12.3 ± 0.96e	6.0 ± 0.1f	3.60 ± 1.00
300–399	57.2 ± 13.1c	52.8 ± 4.96a	3.65 ± 0.35	9.17 ± 1.84	3.45 ± 1.71ab	2340 ± 2140	17.8 ± 0.87d	7.8 ± 0.1e	5.72 ± 2.15
400–499	108 ± 13.7b	35.0 ± 3.85b	ND	9.08 ± 1.67	1.18 ± 0.61b	78.0 ± 69.2	19.0 ± 0.82d	8.5 ± 0.1d	2.77 ± 0.28
500–599	97.2 ± 8.48b	56.4 ± 5.69a	3.38 ± 1.22	10.1 ± 1.29	4.68 ± 2.47ab	1140 ± 938	23.2 ± 0.74c	9.0 ± 0.1c	8.05 ± 3.82
600–699	178 ± 8.71a	33.7 ± 4.88b	ND	9.50 ± 3.82	1.77 ± 1.04ab	2000 ± 1360	23.5 ± 1.09bc	9.5 ± 0.1b	4.85 ± 0.92
700–799	204 ± 14.1a	53.0 ± 9.31a	5.27 ± 3.66	12.9 ± 2.65	8.87 ± 5.99a	9.19 ± 1.50	26.6 ± 1.56ab	10.0 ± 0.1a	4.29 ± 0.96
> 800	208 ± 22.2a	85.3 ± 27.7a	8.83 ± 5.14	19.6 ± 16.2	0.09 ± 0.02ab	8.45 ± 1.89	28.5 ± 2.31a	9.9 ± 0.1a	6.44 ± 1.41

SSA specific surface area, *CEC* cation exchange capacity, *AES* anion exchange capacity, *CCE* calcium carbonate equivalent, *PV* total pore volume, *APS* average particle size, *EC* electrical conductivity, *ND* no data

Different letters within a column for either pyrolysis type, feedstock source, or pyrolysis temperature, indicate a significant difference ($p < 0.05$); no letters present indicate no significant difference

3.1.2 General feedstock choice

Various feedstock sources also influence final biochar properties (Table 1). Wood-based biochars typically contained a greater SSA and PV as compared to other feedstock choices. In terms of SSA and PV, this is a function of reducing relatively large wood-based cell structures to smaller pores and thus increasing overall SSA (Weber and Quicker 2018; Downie et al. 2009) and, consequently, PV. Increasing SSA and PV may also be associated with gas or water volatilization processes during pyrolysis and the loss of micro-molecule organic compounds, both of which can create voids within the biochar matrix during pyrolysis (Guo and Lua 1998). Contrarily, biochars produced from manures/ biosolids typically exhibited relatively low SSA, likely due to the development of deformation, structural cracking or micropore blockage (Ahmad et al. 2014; Lian et al. 2011), along with less distinct porous structures in the feedstock as compared to wood-based biochars.

Crop waste, other grasses, and manures/biosolids biochars had a greater CEC and pH compared to wood-based biochars. CEC can be generated during pyrolysis, as oxygenated surface and inorganic functional groups are formed (Briggs et al. 2012). The increased CEC may also be

attributed to elevated pH leading to pH-dependent charge, or insoluble precipitates present in the ash that act as reaction sites (Ippolito et al. 2017). Others have related increased CEC to increases in SSA (Kloss et al. 2012; Qambrani et al. 2017; Liang et al. 2006), yet the data presented here contradict these findings. Concomitant with increasing ash content from wood, to crop, to other leafy-grassy, to manures/biosolids biochars, the CCE is also greatest in manure- biosolids-derived biochars. This is likely due to oxide and hydroxide mineral phase precipitation during pyrolysis (e.g., Ippolito et al. 2012).

3.1.3 Pyrolysis temperature

Increasing pyrolysis temperature also influences final biochar composition (Table 1).

Specific surface area increased with increasing pyrolysis temperature, as shown by others (Domingues et al. 2017; Luo et al. 2015). This is a function of shrinking the solid matrix, causing relatively large pores to become smaller and thus increasing overall SSA (Weber and Quicker 2018; de Mendonça et al. 2017). Surface area has been previously correlated with sorption/retention of nutrients and contaminants, while pore volume (which, in general increases with

pyrolysis temperature) is assumed to affect water availability and soil aeration (Ajayi and Horn 2016; Qambrani et al. 2017). Increasing pyrolysis temperature also clearly increased biochar ash content and pH, as solid phase hydroxide and carbonate phases increase within the ash, causing pH values to concomitantly increase. This concept is described in more detail in the biochar physicochemical correlations, Sect. 3.1.4 below.

3.1.4 Biochar physicochemical correlations

Correlations between biochar pH and ash content, pyrolysis temperature and pH, and pyrolysis temperature and SSA, based on all pertinent data collected, are shown in Fig. 1. Increasing biochar pH generally correlates with an increase in ash content (Fig. 1a) as also shown by Lehmann (2007). This correlation could be useful for practitioners designing pyrolysis systems for creating biochars needed for soil liming purposes (e.g., in acidic or acid generating mines soils; Ippolito et al. 2017; Sigua et al. 2019; Godlewska et al. 2017). Increasing pyrolysis temperature caused biochar pH to increase (Fig. 1b), likely due to loss of acidic functional groups (Novak et al. 2009) and the formation of Ca- Mg-, Na-, and K-bearing oxide, hydroxide, and carbonate mineral phases (Cao and Harris 2010) that can raise the pH to ranges extending from 9.9 to 13 (aqion 2019). Ngatia et al. (2017) also illustrated biochar pH correlations to alkali earth elements such as those mentioned above. Increasing pyrolysis temperature also increased biochar specific surface area (Fig. 1c), as observed by others (e.g., Lu et al. 2012; Hass et al. 2012). Increasing specific surface area appears to be a function of decreases in cell pore diameter (Ahmad et al. 2012), along with tar, oils, H and O removal with increasing pyrolysis temperatures (Kloss et al. 2012; Chen et al. 2008).

4 Biochar total elemental analysis

4.1 Pyrolysis type, general feedstock choice, and pyrolysis temperature

Changes in biochar total macro-elements as a function of pyrolysis type, general feedstock choice, and pyrolysis temperature, are shown in Table 2. Fast pyrolysis favored total S, K, Ca, and Mg content as compared to slow pyrolysis. However, in general, pyrolysis type had little influence on total macro-elements as compared to feedstock choice and temperature; total macro-elements have been previously correlated with feedstock choice and pyrolysis temperature (Zhang et al. 2017b). In terms of feedstock choice, wood-based feedstocks led to greater C content over other feedstock choices. If C storage was a goal, wood-based biochars, especially with high aromatic-C character (Wang et al. 2016)

and low O/C and H/C ratios (Spokas 2010) should be applied to soils. Grass-based feedstocks contained relatively elevated K and Ca content as compared to other feedstocks, while manures/biosolids-based feedstocks contained the greatest N, S, P, Ca, and Mg concentrations over biochars from other feedstocks, similar to findings by Amoah-Antwi et al. (2020). At first glance, it appears that if N–P–K fertilizer use was a goal, grass- or manure/biosolids-based biochars could be utilized (Lin et al. 2017; Gondek and Mierzwa-Hersztek 2016; Wang et al. 2013; Brewer et al. 2012); this concept is revised within the context of specific feedstock choices in Sect. 6.5 below. In terms of pyrolysis temperature, increasing temperature increased C, P, Ca, and Mg concentrations, also as suggested by Chen et al. (2016). Specifics, with respect to biochar total elemental analysis, are also discussed below.

4.2 Carbon, hydrogen, and oxygen

For biochars, total C content is often elevated as most feedstocks contain appreciable C concentrations, yet feedstock choice significantly affects biochar C content (Table 2). Wood-based biochars contained greater C as compared to biochars made from other feedstock choices, simply due to a lack of other elements (e.g., N, S, P, K, Ca, and P) leading to a smaller C-dilution effect in wood-based biochars.

Biochar C compounds can be grouped into relatively condensed (i.e., stable, non-mineralizable) aromatic C compounds, compared to easier-degradable, micro-molecular or water-soluble C (Lehmann et al. 2011). During pyrolysis, dehydration, cleavage, and polymerase reactions cause easily degradable C compounds to be restructured, while other elements may be lost to volatilization, and thus overall biochar total C content increases with increasing pyrolysis temperature (Weber and Quicker 2018; Antal and Grønli 2003; Table 2). Biochar C bioavailability is temperature dependent, with higher pyrolysis temperatures related to larger non-labile C fractions (Nelissen et al. 2012). Greater pyrolysis temperatures tend to create relatively stable, aromatic C compounds and silicate–carbon complexes that are usually regarded as recalcitrant to microbial oxidation (Guo and Chen 2014). When placed in soils, recalcitrant C could last hundreds to thousands of years, and as such, biochar land application may play a role in climate mitigation (Schmidt et al. 2019; Werner et al. 2018; Woolf et al. 2018; Bolan et al. 2012).

Increasing pyrolysis temperature significantly increased biochar C content via volatilization losses of other elements, especially H and O (Table 2). As pyrolysis temperature increases, water, organic surface functional groups, and tars are lost, all of which contain H and O atoms (Ahmad et al. 2014; Cantrell and Martin 2012). During pyrolysis, O is released at a greater rate than H, with the final biochar

Fig. 1 The relationship between **a** pH and ash content, **b** pyrolysis temperature and pH, and **c** pyrolysis temperature and specific surface area
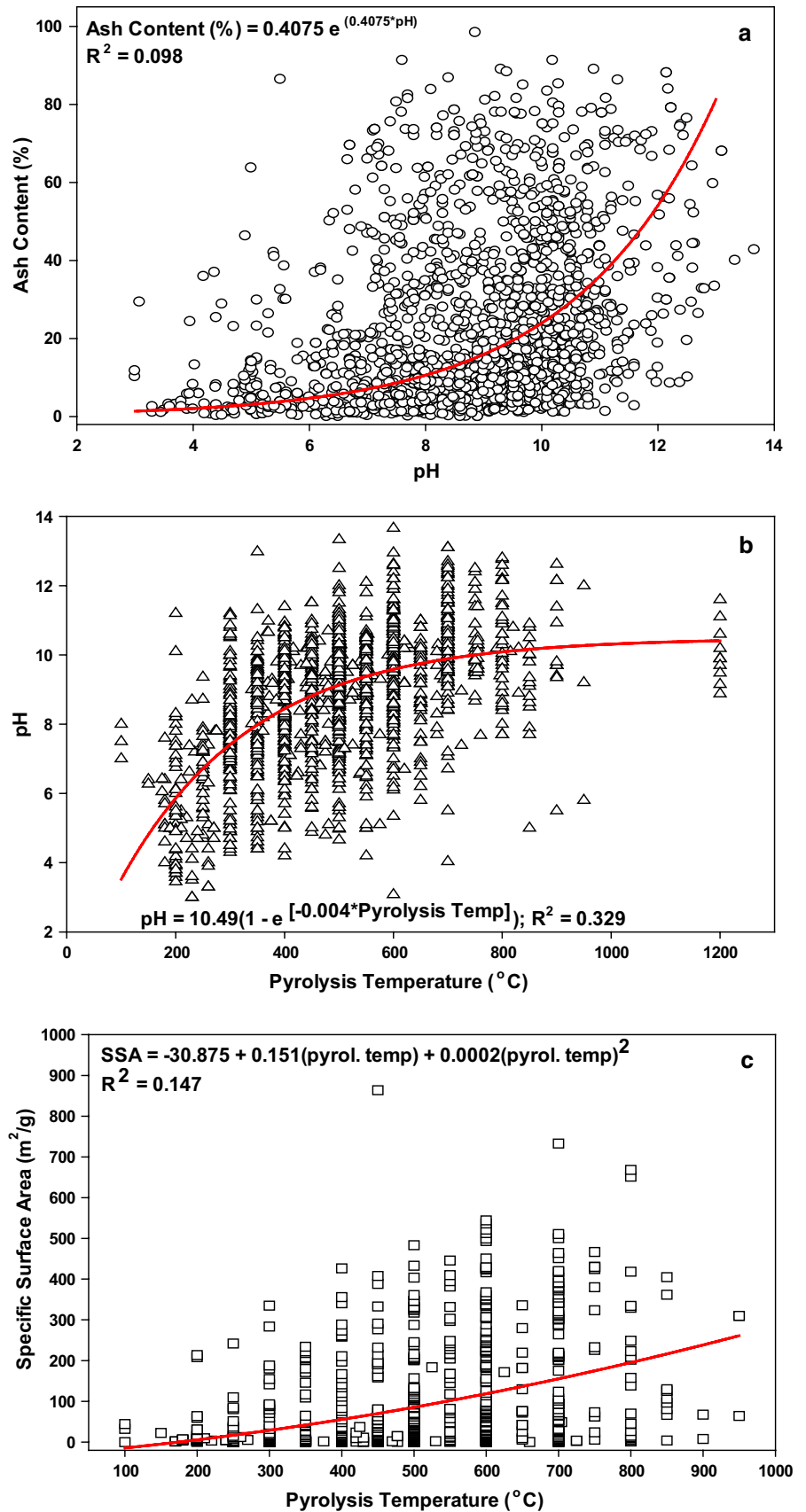
Table 2 Biochar mean total macro-element concentrations (±standard error of the mean) based on pyrolysis type, feedstock source, and pyrolysis temperature, on a dry weight basis

	C	H	O	N	S	P	K	Ca	Mg
	(%)				(g kg^{-1})				
Pyrolysis type									
Fast	60.6 ± 0.47	3.37 ± 0.08	19.1 ± 0.38	1.63 ± 0.06	0.85 ± 0.09a	14.2 ± 0.72	46.8 ± 4.69a	44.3 ± 4.01a	43.5 ± 12.1a
Slow	60.8 ± 0.34	3.36 ± 0.09	18.4 ± 0.29	1.63 ± 0.04	0.55 ± 0.04b	12.0 ± 0.56	22.8 ± 1.33b	29.1 ± 1.68b	5.73 ± 0.30b
Feedstock source									
Wood based	70.5 ± 0.39a	3.38 ± 0.08b	17.7 ± 0.35bc	0.95 ± 0.03d	0.44 ± 0.07b	4.00 ± 0.46d	19.3 ± 2.62c	26.3 ± 2.60b	5.18 ± 0.84b
Crop wastes	61.4 ± 0.41c	3.28 ± 0.10b	18.1 ± 0.38b	1.54 ± 0.06c	0.39 ± 0.06b	8.00 ± 0.97c	40.9 ± 3.62b	20.7 ± 2.16b	6.06 ± 0.76b
Other grasses	63.6 ± 0.72b	5.11 ± 0.50a	20.9 ± 0.74a	1.80 ± 0.14b	0.51 ± 0.21b	20.1 ± 6.08b	59.1 ± 12.2a	45.9 ± 12.0a	34.3 ± 12.7b
Manures/ Biosolids	41.6 ± 0.68d	2.73 ± 0.10c	16.5 ± 0.70c	2.42 ± 0.06a	0.89 ± 0.06a	25.7 ± 1.44a	25.3 ± 1.79c	52.7 ± 3.64a	57.8 ± 20.5a
Pyrolysis Temp (°C)									
< 300	54.1 ± 0.59e	5.62 ± 0.25a	30.6 ± 0.60a	1.70 ± 0.10ab	0.43 ± 0.06	9.03 ± 1.32b	26.7 ± 5.24	25.0 ± 4.67bc	5.41 ± 0.88ab
300–399	58.0 ± 0.58d	4.70 ± 0.24b	23.6 ± 0.50b	1.81 ± 0.09a	0.44 ± 0.07	9.60 ± 1.56b	23.8 ± 4.04	23.0 ± 4.03c	43.0 ± 22.1a
400–499	62.3 ± 0.59bc	3.78 ± 0.19c	18.1 ± 0.41c	1.61 ± 0.08b	0.54 ± 0.08	10.1 ± 1.40b	32.7 ± 3.93	34.7 ± 4.80bc	9.61 ± 3.44ab
500–599	62.5 ± 0.59bc	2.83 ± 0.09d	14.2 ± 0.40d	1.34 ± 0.04c	0.54 ± 0.09	11.8 ± 1.36b	32.6 ± 3.93	28.6 ± 2.84c	24.3 ± 9.22b
600–699	65.8 ± 0.87a	2.31 ± 0.11e	12.7 ± 0.52e	1.32 ± 0.07c	0.60 ± 0.10	12.6 ± 2.29b	26.8 ± 4.93	36.0 ± 5.25abc	9.87 ± 3.51ab
700–799	64.7 ± 1.30ab	1.77 ± 0.12ef	13.0 ± 0.90de	1.26 ± 0.07c	0.63 ± 0.14	18.8 ± 2.49a	34.1 ± 8.68	43.0 ± 6.42ab	10.1 ± 4.25ab
> 800	61.0 ± 1.82c	1.45 ± 0.12f	9.51 ± 1.00f	1.51 ± 0.26abc	0.36 ± 0.07	14.5 ± 3.68ab	34.5 ± 6.21	54.1 ± 11.8a	12.7 ± 3.50ab

Different letters within a column for either pyrolysis type, feedstock source, or pyrolysis temperature, indicate a significant difference ($p < 0.05$); no letters present indicate no significant difference

product characterized by a decrease in H/C-ratio and containing low oxygen-content. Thus, understanding the ratios between H, C, and O, as depicted in the Van-Krevelen diagram, may be useful for discerning biochar longevity in soil systems (Schimmelpfennig and Glaser 2012; Spokas 2010).

Specifically, the atomic ratios of O/C to H/C have been used to describe the pyrolysis carbonization process (Weber and Quicker 2018), and more specifically to describe several key biochar environmental longevity factors as a function of these ratios. Figure 2 illustrates how the O/C and H/C

Fig. 2 The relationship between the molar ratio of O/C and H/C and pyrolysis temperature (Van Krevelen Diagram). Biochars with O/C ratios < 0.2 are highly stable (half-life > 1000 years), between 0.2 and 0.6 are moderately stable (half-life between 100 and 1000 years), and > 0.6 are relatively unstable (half-life less than 100 years; Spokas 2010). Biochars with H/C ratios < 0.7 have greater fused aromatic ring structures and have been thermochemically altered as compared to biochars with H/C ratios > 0.7 (IBI 2015)
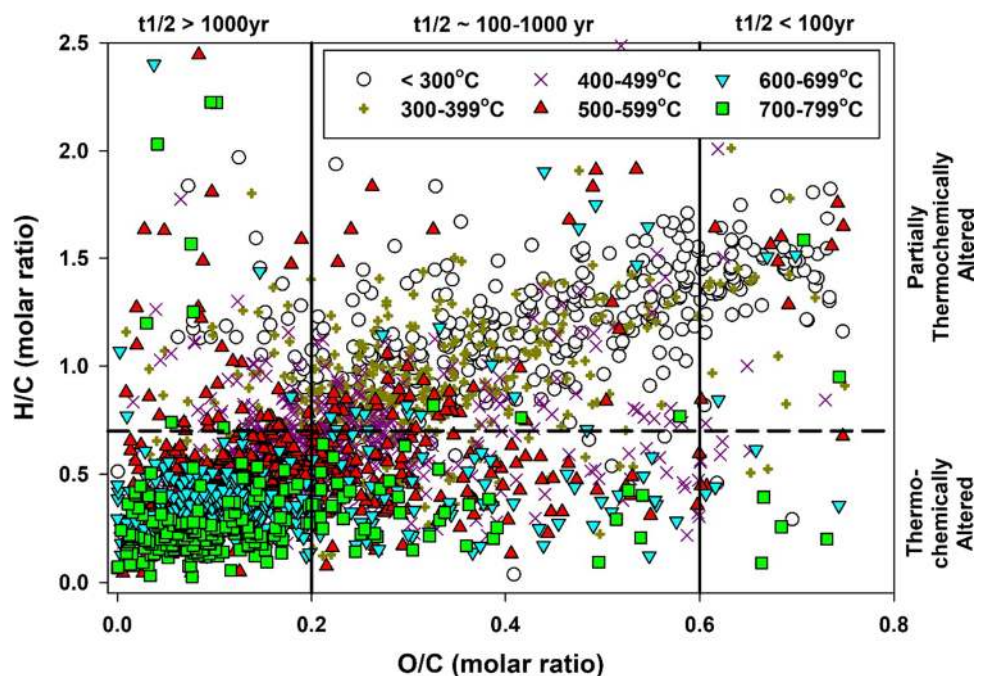
ratios are altered as a function of pyrolysis temperature. Spokas (2010) described biochars with O/C ratios: (a) < 0.2 as highly stable (half-life > 1000 years); (b) between 0.2 and 0.6 as moderately stable (half-life between 100 and 1000 years); and (c) > 0.6 as relatively unstable (half-life less than 100 years). Meanwhile, biochars with H/C ratios < 0.7 have greater fused aromatic ring structures and have been thermochemically altered as compared to biochars with H/C ratios > 0.7 (IBI 2015). Biochar H/C ratio has been also found to be a key factor defining its N_2O mitigation potential, with biochars with H/C ratios < 0.3 being the most effective (Cayuela et al. 2015). Based on the above information and the data presented in Fig. 2, biochars created at pyrolysis temperatures > 600 °C would typically be the most recalcitrant when placed in soils and, at the same time, among the most effective in mitigating N_2O emissions (e.g., see: Borchard et al. 2018; Cayuela et al. 2015). Biochars created between 500 °C and 599 °C would typically have half-lives of 100–1000 years when placed in soils (Pariyar et al. 2020). Biochars created at temperatures < 500 °C should have relatively lower half-lives when placed in soils due to these materials only being partially thermochemically altered (e.g., see Table 2 in Spokas 2010). Similar observations have been found by Wolf et al. (2013) when combusting various feedstocks over increasing temperatures. Comparing 128 observations from 24 studies, Wang et al. (2016) found that the mean residence time of recalcitrant biochar C pools was 556 years. It is obvious that understanding pyrolysis temperature is important for the C sequestration potential of biochar (Wang et al. 2016).

4.3 Total macro-nutrient concentrations

Total N and P contents are comparable between slow and fast pyrolysis, yet fast pyrolysis favored greater S, K, Ca, and Mg concentrations (Table 2). Feedstock choice dictated total N content, in the order of wood biochars < crop waste biochars < other grasses < manures/biosolids biochars. Greater biochar N content is likely a function of greater amino acids and proteins present in these materials (Tsai et al. 2012). As suggested by Cantrell et al. (2012), this provides an advantage to greater N-containing biochars, such as manures/biosolids biochars, to act as a fertilizer (e.g., N) source. Contrarily, substantial N amounts are released as gaseous forms (e.g., NO, N_2O, NO_2, NH_3, N_2; > 60%) with increasing pyrolysis temperature as illustrated in Table 2. The same response, at the same temperatures, were reported by Ippolito et al. (2015) when comparing pyrolysis temperature effects on N within a smaller biochar dataset ($n < 100$).

Feedstock choice has been noted to typically be the primary determinant on biochar total S content (Cheah et al. 2014); our meta-analysis results suggest that only manures/biosolids-based biochars contain a greater S content as compared to biochars made from other feedstocks (Table 2). Biochars containing elevated S content (e.g., manures; Sager 2012) have been shown to increase soil S bioavailability (Blum et al. 2013). Relatively lower pyrolysis temperatures (e.g., < 500 °C) have been shown to keep total biochar S content intact, yet greater temperatures can lead to gaseous S losses (Wang et al. 2013). However, data presented in Table 2 do not support this contention, showing no significant difference in S content when varying pyrolysis temperature. Pyrolysis temperature has also been shown to be a main determinant of the S forms found in biochar. Biochar S is mainly found in the organic fraction, such as dibenzothiophene (59% of total sulfur) and dibenzyldisulfide (14% of total sulfur), both of which can be bound to biochar-borne C (Cheah et al. 2014). As pyrolysis temperature increases, these organic-S bearing phases are converted to gases and lost (Carpenter et al. 2010). However, some S still remains, likely in a recalcitrant form bound to Ca, K, Mg, and Si at higher pyrolysis temperatures (> 800 °C) (Knudsen et al. 2004). Perhaps S data presented in Table 2 reflect these recalcitrant S forms present with respect to increasing pyrolysis temperature.

Biochar total P, K, Ca, and Mg concentrations are also affected by feedstock choice (Table 2). Manures/biosolids-based biochars typically contained greater P, Ca, and Mg concentrations, other grass-based biochars contained appreciable K and Ca, while crop wastes- and wood-based biochars contained the least quantities of these four elements. In general, increasing pyrolysis temperature increased P and Ca content, had mixed effects with respect to Mg content, and had no significant impact on K concentration. The P, K, Ca, and Mg feedstock and pyrolysis temperature findings are likely a result of the initial elemental concentrations present in various feedstock, as well as increasing ash content with increasing pyrolysis temperature (Table 1). As ash content increases, Ca oxides, hydroxides, and carbonate mineral phases precipitate, which leads to increased total Ca concentration. In terms of P, as pyrolysis temperature increases biochar P content typically increases as well (e.g., Ippolito et al. 2015), likely due to P forming associations with carbonate phases. Although not strongly illustrated in Table 2, it is important to note that P-containing compounds can volatilize above 760 °C (Knicker 2007) causing total P concentrations to decrease.

4.4 Total micro-nutrient concentrations

Biochar total micro-nutrient concentrations, based on pyrolysis type, feedstock source, and pyrolysis temperature, are shown in Table 3. Only total Cu and Zn concentrations were affected by pyrolysis type, with fast pyrolysis favoring greater concentrations over slow pyrolysis. As with total macro-nutrient concentrations, total

Table 3 Biochar mean total micro-element concentrations (± standard error of the mean) based on pyrolysis type, feedstock source, and pyrolysis temperature, on a dry weight basis

	Fe (g kg^{-1})	Cu	Zn	B	Mn (mg kg^{-1})	Mo	Co	Cl
Pyrolysis type								
Fast	7.74 ± 1.76	314 ± 77.0a	1140 ± 236a	20.7 ± 3.36	391 ± 47.1	4.37 ± 0.90	5.51 ± 0.89	3140 ± 527
Slow	7.53 ± 0.89	159 ± 15.9b	356 ± 32.4b	32.2 ± 5.78	383 ± 28.4	3.22 ± 0.75	4.02 ± 0.82	4390 ± 648
Feedstock source								
Wood based	2.72 ± 0.37b	53.7 ± 10.4b	406 ± 144b	15.5 ± 3.13a	227 ± 24.2c	1.12 ± 0.37b	2.17 ± 0.67b	1060 ± 176c
Crop wastes	3.84 ± 0.52b	52.3 ± 14.8b	152 ± 43.9b	13.8 ± 2.65a	353 ± 58.6b	2.23 ± 0.65b	4.09 ± 1.52ab	4760 ± 848b
Other grasses	3.64 ± 0.86b	65.6 ± 21.0b	123 ± 24.5b	9.48 ± 4.31a	348 ± 62.5bc	0.80 ± 0.24b	0.48 ± 0.15b	3020 ± 1,560bc
Manures/Biosolids	21.6 ± 3.83a	565 ± 92.4a	946 ± 76.9a	57.7 ± 11.0b	584 ± 49.6a	6.96 ± 1.26a	6.27 ± 1.03a	10,050 ± 1,300a
Pyrolysis temp (°C)								
< 300	8.86 ± 2.91	873 ± 469a	431 ± 191a	55.7 ± 27.8ab	71.5 ± 37.5bc	0.38 ± 0.23	ND	2830 ± 779b
300–399	3.21 ± 1.27	177 ± 50.0b	260 ± 48.0b	33.2 ± 12.3ab	236 ± 45.9c	2.49 ± 1.36	1.88 ± 1.31	1810 ± 1,130b
400–499	8.36 ± 2.86	213 ± 44.5b	864 ± 256a	39.2 ± 8.51a	412 ± 64.2b	3.32 ± 1.17	4.28 ± 1.10	4190 ± 1,080ab
500–599	7.71 ± 1.93	176 ± 34.9b	392 ± 42.5b	26.8 ± 4.72ab	356 ± 32.2bc	3.59 ± 0.66	4.06 ± 1.03	3150 ± 848b
600–699	8.63 ± 2.38	169 ± 60.9b	414 ± 95.1b	23.2 ± 6.14ab	337 ± 54.4bc	0.75 ± 0.38	3.85 ± 1.22	6090 ± 1,280a
700–799	9.44 ± 3.38	301 ± 113b	343 ± 88.7b	21.0 ± 13.9ab	348 ± 87.9bc	4.60 ± 4.35	6.05 ± 3.95	2290 ± 780b
> 800	9.38 ± 3.17	162 ± 45.4b	779 ± 215a	10.4 ± 5.14b	685 ± 206a	ND[†]	ND	4520 ± 1,520ab

Different letters within a column for either pyrolysis type, feedstock source, or pyrolysis temperature, indicate a significant difference ($p < 0.05$); no letters present indicate no significant difference

micro-nutrient concentrations were almost always significantly greater in manures/biosolids-based biochars as compared to other biochars. This is a function of manures/biosolids feedstocks being fortified with micro-nutrients that were not assimilated by livestock or as a waste product from municipal/industrial sources (Sistani and Novak 2006). Thus, manure-based feedstocks contain inherently greater micro-nutrient concentrations than other feedstocks. This could also be a function of ash content present based on feedstock choice (Table 1) creating micro-nutrient oxide, hydroxide, and carbonate phases (e.g., CuO, $Cu(OH)_2$, or $CuCO_3$; Ippolito et al. 2012; Zhang et al. 2017a). Likewise, increasing pyrolysis temperature was shown to affect ash content (Table 1), with relatively similar connections to increasing micro-nutrient concentrations as a function of temperature (Table 3).

Increasing micro-nutrient concentrations within biochars suggest that they may be used as a micro-nutrient fertilizer source. Chang et al. (2015) showed that a biochar containing Fe, Cu, Zn, Mn, and Co could potentially be used to supply micro-nutrients to plants. More specifically, Sigua et al. (2016) utilized poultry litter biochar addition to soil, observing an increase in extractable Fe, Mn, Cu and Zn by 19, 46, 68 and 32%, respectively, as compared to a control. Additionally, Zhao et al. (2018) reported that although a pig manure biochar contained excessive total Mn (1230 mg kg^{-1}), Cu (780 mg kg^{-1}),

and Zn (1010 mg kg^{-1}), their bioavailability was up to several orders of magnitude lower.

5 Biochar available nutrient analysis as a function of pyrolysis type, feedstock, and pyrolysis temperature

Biochar total elemental analysis only describes maximum nutrient concentrations present, which is not truly indicative of the nutrient availability when applied to soil. Available nutrients are those elements that may be readily absorbed by plants, as determined using various extractants (e.g., water, 1 M KCl, 0.01 M $CaCl_2$, DTPA, Morgan, Mehlich, or Olsen extracting solutions). Although these extractants were originally developed for use in soils, they have been widely used with other soil amendments, including biochars and in biochar-amended soils (e.g., Lehmann et al. 2003; Lentz and Ippolito 2012). Changes in biochar available macro- and micro-elements, as a function of pyrolysis type, feedstock choice, and pyrolysis temperature, are shown in Table 4.

5.1 Pyrolysis type

Out of the ten available nutrients studied, only two were affected by pyrolysis type (Table 4). Biochars created via slow pyrolysis favored greater Fe and NO_3 availability over

Table 4 Biochar mean available macro- and micro-element concentrations (extracted with either H$_2$O, 1 M KCl, 0.01 M CaCl$_2$, DTPA, Morgan, Mehlich, or Olsen extracting solutions; ± standard error of the mean) based on pyrolysis type, feedstock source, and pyrolysis temperature, on a dry weight basis

	P	K	Mg	Ca	Fe	Mn	Zn	Cu	NO$_3^-$	NH$_4^+$
					(mg kg^{-1})					
Pyrolysis type										
Fast	404.0±145	4490±720	450±90.6	1670±382	22.2±7.90b	34.9±11.8	60.6±24.3	4.27±1.89	19.8±3.40b	265±106
Slow	640.5±117	6050±686	675±102	2450±365	290±59.8a	28.9±8.20	30.4±5.90	9.21±3.78	66.4±19.9a	295±185
Feedstock source										
Wood based	118±17b	1660±289d	232±43.4b	1780±444b	134±53.3	19.6±3.8b	39.1±28.6c	3.3±0.9b	32.0±10.7b	16.3±4.5b
Crop wastes	517±125b	9019±1,220b	722±137a	1285±185b	309±95.0	26.0±9.2b	15.3±3.5c	1.9±0.5b	15.7±3.1b	43.9±12.3b
Other grasses	411±57b	16,290±3,140a	1060±617a	1410±351b	0.5±0.1	3.6±1.1b	0.5±0.3d	2.7±2.5b	9.8±6.7b	14.4±5.2b
Manures/Biosolids	1380±369a	4316±670c	993±230a	4488±1,000a	68.4±23.1	79.9±34.3a	91.4±17.4a	20.7±11.4a	143.7±54.8a	1005±472a
Pyrolysis temp (°C)										
< 300	25.1±9.72c	1120±730b	132±45.9b	195±53.9b	29.2±15.1	6.38±2.30	1.52±0.67	1.02±0.24	65.6±39.6	67.2±24.4
300–399	517±183b	4930±997b	641±189b	2180±780a	216±94.0	40.8±23.9	2.85±1.07	6.35±3.77	99.4±51.7	722±303
400–499	424±162c	3810±637b	492±107b	1930±515a	188±82.0	31.1±7.77	62.7±33.6	2.17±0.61	44.9±30.8	801±570
500–599	682±214b	6480±1,030b	480±111b	1920±475b	215±107	18.9±7.56	42.4±10.5	16.6±12.8	38.8±17.2	40.0±13.6
600–699	365±86.1b	5010±1,420b	747±239b	3130±989a	133±46.5	41.4±19.7	34.4±15.8	7.85±2.47	72.8±64.9	81.1±36.6
700–799	1230±575a	13,420±4,400a	1510±616a	3270±1,040a	85.4±44.7	73.2±62.7	52.6±37.8	8.80±3.29	58.4±55.5	43.4±39.0
> 800	245±105b	5580±2,310a	537±422a	1300±599a	6.55±3.95	2.05±0.95	0.45±0.35	0.25±0.15	7.48±3.40	35.0±17.6

Different letters within a column for either pyrolysis type, feedstock source, or pyrolysis temperature, indicate a significant difference ($p < 0.05$); no letters present indicate no significant difference

fast pyrolysis. Depending on the extractant used, nutrient availability may be either over- or under-estimated (e.g., the use of Morgan or Mehlich extractants, which contain weak acids, for use with alkaline-containing materials could over-estimate availability). In the current study, we grouped all data together and did not model effect of extractants used for nutrient availability determination; this would be worth exploring in the future.

5.2 Feedstock choice

In general, manure/biosolids-based biochars typically contained the greatest available nutrient concentrations as compared to other biochars (Table 4). This is not surprising given that these feedstocks contain, overall, greater nutrient contents as compared to other feedstocks (e.g., Williams et al. 2017). All other feedstock-based biochars generally were grouped together in terms of nutrient availability, potentially a consequence of lower ash content leading to lower nutrient retention (e.g., Williams et al. 2016).

5.3 Pyrolysis temperature

Increasing pyrolysis temperature increased only the macro-elements P, K, Mg, and Ca (Table 4). As mentioned in the biochar total elemental analysis discussion (Sect. 4, above), as pyrolysis temperature increases, water, volatile bio-oil compounds, acids, organic surface functional groups and tars are lost, all of which contain H and O resulting in their losses as well (Ahmad et al. 2014; Cantrell and Martin 2012; Antal and Grønli 2003). This concentrates other elements in the final product, with macro-nutrient availability appearing to be a function of pyrolysis temperature. This concept is explored in more detail below.

6 Available nutrient analysis correlations

Ippolito et al. (2015) suggested that total elements present in biochars cannot accurately predict nutrient availability. However, their dataset utilized was based only on approximately 80 published biochar articles. It is worth to revisit this concept, as well as other correlations, based on nearly 5400 published articles reviewed in the current study. Thus, Pearson correlations between biochar available and total nutrient contents, pyrolysis temperature, pyrolysis type, or feedstock choice were first determined (Table 5). Most coefficients were not significant. However, some exceptions were present for predicting biochar nutrient availability based on total nutrient content, such as for K and Cu. Predicting biochar nutrient content solely on pyrolysis temperature or production technique appears poor; predicting nutrient

Table 5 Pearson correlation coefficients between available N, P, K, Ca, Mg, Fe, and Cu and total nutrient concentration, pyrolysis temperature, pyrolysis type, and feedstock choice

Available nutrient content	Total nutrient content	Pyrolysis temperature	Pyrolysis type	Feedstock choice
N	*0.267*	− 0.074	0.029	*0.167*
P	0.110	0.135	0.130	*0.275*
K	*0.422*	*0.191*	− 0.122	*0.190*
Ca	*0.331*	0.052	0.140	*0.323*
Mg	0.022	0.123	0.100	*0.200*
Fe	*0.301*	0.107	*0.414*	− 0.020
Cu	*0.669*	0.028	0.104	0.206

Bold, italicized numbers indicate significance ($p < 0.05$)

availability based on feedstock choice appears somewhat more promising.

However, in order to parse the data into something meaningful for the end-user, presented below are comparisons between total and available nutrients with respect to all biochar data, fast or slow pyrolysis, pyrolysis temperature, and feedstock choice. Only data where both total and available nutrients were presented (N, P, K, Ca, Mg, Fe, and Cu) in previously published works are shown.

6.1 All data: effects on nutrient availability

The total versus available N, P, K, Ca, Mg, Fe, and Cu data, for the complete dataset for each element, are presented in Figures S1A through S1G. The data suggest that predicting biochar plant-available concentrations from total elemental content is relatively poor for most elements ($R^2 = 0.19$, 0.01, 0.35, 0.11, no fit, and 0.09 for N, P, K, Ca, Mg, and Fe, respectively). However, predicting plant-available biochar Cu from total Cu content had an $R^2 = 0.97$ utilizing an exponential growth model. Unfortunately, most biochar producers and end-product users are likely not as concerned about applying plant-available Cu to soils via biochar application as compared to other macro-element availability.

In terms of macro-element availability, most end-product users would likely be concerned about N availability and whether they need to add supplemental N fertilizers with biochars to offset potential negative crop N responses (e.g., Borchard et al. 2014; Lentz and Ippolito 2012). For example, in the western US, irrigated winter wheat or corn could require 85 and 235 kg N ha^{-1}, respectively, to maximize yields (Davis and Westfall 2014a, b). The NO_3 and NH_4 data in Table 4, along with data shown in Figure S1A, suggest that most biochars (except manures/biosolids biochars) contain available N contents below ~200 mg kg^{-1}; at 200 mg of available N kg^{-1} biochar, an end-user might need to apply between 425 and 1175 Mg biochar ha^{-1} to supply the N

demands of winter wheat or corn, respectively. Unfortunately, microbial immobilization should also be accounted for, which would likely limit N availability, as described by Borchard et al. (2014). Furthermore, these biochar application rates to soils would equal ~19% and 52% by weight, well over the general application guidelines many biochar researchers are considering (~0.5% to 1% by weight, or 112 to 224 Mg ha^{-1}). If biochar costs are considered (e.g., $500–$1000 USD Mg^{-1}), crop-land applications would be economically unrealistic if it was just for an N fertilization effect (that is not given in woody biochars anyway due to the N being bound into the biochar matrix). Biochars would need to contain 2000 mg of available N kg^{-1}, or greater, to bring application rates near the 0.5–1% application level. According to data presented in Table 4 and Figure S1A, very few untreated biochars meet this requirement. Apart from N, taking a closer look into varying pyrolysis type, temperature, or feedstock choice may provide additional insight into overall biochar nutrient availability prediction.

There may be ways to increase the ability of biochar to provide plant-available N, even though NO_3 and NH_4 content of freshly produced biochar is near-zero (e.g. Kammann et al. 2015; Haider et al. 2016). Biochar has the ability to capture NO_3 when co-composted (Hagemann et al. 2017a, (b); wood biochars have been shown to release up to 5000 mg NO_3 kg^{-1} following co-composting when repeatedly extracted (Kammann et al. 2015; Haider et al. 2016; Hagemann et al. 2017b). Biochar can also capture available N when biochar resides in soils for longer time periods (Haider et al. 2016, 2017). In organic environments with alternating moisture regimes, an organo-mineral coating forms on biochar surfaces (Hagemann et al. 2017a). The coating is enriched in functional groups that improve the ability of biochar to capture and release nitrate (and to a lesser extent ammonium) (Kammann et al. 2015; Hagemann et al. 2017a). The mechanism, however, is not yet completely understood (Joseph et al. 2017) and deserves further attention.

6.2 Fast pyrolysis effects on nutrient availability

The effect of fast pyrolysis on the correlation between total and available biochar nutrients are presented in Figures S2. As compared to all data (Figure S1), separating data by fast pyrolysis did not increase the predictive fit for most elements, and in some cases decreased the degree of fit. This suggests that predicting biochar nutrient availability based on fast pyrolysis is relatively poor. However, predicting available Cu based on total Cu in fast pyrolysis biochars still has a relatively good fit ($R^2 = 0.74$; exponential growth model). Unfortunately, as previously mentioned, most biochar end-users likely would not be concerned with Cu availability.

6.3 Slow pyrolysis effects on nutrient availability

The effect of slow pyrolysis on the correlation between total and available biochar nutrients are presented in Figures S3. As compared to all data (Figure S1), separating data by slow pyrolysis increased the predictive fit for most elements. Furthermore, slow pyrolysis tended to fit data to a greater degree than fast pyrolysis. This may simply be due to the larger number of biochars created from slow pyrolysis as compared to fast pyrolysis, with gaps in the data reduced simply due to more literature information. Fitting biochar available nutrient to total nutrient content from fast to slow pyrolysis improved the predictive R^2 function for P (0.05–0.13), K (0.32–0.47), Ca (0.25–0.46), Mg (0.03–0.29), and Cu (0.74–0.98). Although these fits might not be perfect, the data suggest that predicting slow pyrolysis biochar's plant-available nutrient content, based on total nutrient content, is not out of the question (e.g., K, Ca, and Cu).

6.4 Pyrolysis temperature effects on nutrient availability

The effects of pyrolysis temperature (from < 300 °C to > 800 °C) on the correlation between total and available biochar nutrients are presented in Figures S4. In general, available K, Mg, and Fe content appear to increase with increasing pyrolysis temperature, then decrease with further rising pyrolysis temperatures > 800 °C. It also appears that, in general, temperatures < 300 °C or > 800 °C produce biochars with low available nutrient content.

6.5 Specific feedstock choice effects on nutrient availability

Based on Pearson correlations (Table 5), predicting biochar nutrient availability on feedstock choice appears somewhat promising. The effect of feedstock choice on the correlation between total and available biochar primary macro-nutrients (N, P, and K) are presented in Table 6, while all nutrient data (where both total and available nutrients were reported) are presented in Figures S5. The discussion below focuses solely on the predicted availability of N, P, and K in biochars created from specific feedstocks. However, the reader is encouraged to visit the supplemental figures for details regarding predicting N, P, K, Ca, Mg, Fe, and Cu availability.

6.5.1 Wood-based feedstocks

Previous research has focused a great deal of attention on utilizing hardwood and softwood feedstocks for biochar creation as compared to other materials. Based on a smaller dataset analyzed, Ippolito et al. (2015) showed that hardwood biochars would supply less than 0.002% of the total

Table 6 Regression analysis results of best fits (based on linear, quadratic, exponential rise to a maximum, or exponential growth equations) for available N, P, and K based on total concentrations as a function of feedstock choice; number of observations; R^2 value

Feedstock	Available N = ; n; R^2	Available P = ; n; R^2	Available K = ; n; R^2
Hardwoods	$31.3 - 29.1(\text{Total N}) + 33.5(\text{Total N})^2$; 74; 0.12	$251(1 - e^{(-0.005 \times \text{Total P})}$; 74; 0.12	$-883 + 0.50(\text{Total K})$; 31; 0.87
Softwoods	$44.0 - 126(\text{Total N}) + 57.7(\text{Total N})^2$; 35; 0.68	$43.8(1 - e^{-0.008 \times \text{Total P}})$; 24; 0.08	$41.3 + 0.313(\text{Total K})$; 23; 0.54
Corn stalks/Cobs	$40.2 - 55.8(\text{Total N}) + 20.3(\text{Total N})^2$; 9; 0.41	$-154 + 0.36(\text{Total P})$; 5; 0.48	$-3910 + 0.669(\text{Total K})$; 13; 0.33
Wheat straw	$74.5 - 14.5(\text{Total N})$; 11; 0.09	$83.4 + 0.009(\text{Total P})$; 12; 0.82	$6010 + 0.042(\text{Total K})$; 10; 0.66
Rice straw/Husks	$3.95 + 43.8(\text{Total N})$; 19; 0.02	$-103 + 0.29(\text{Total P})$; 11; 0.50	No Fit
Poultry manure	$-494 + 272(\text{Total N})$; 17; 0.11	$434 + 0.027(\text{Total P})$; 22; 0.07	No Fit
Pig manure	$e^{(1.99 \times \text{Total N})}$; 8; 0.99	$-686 + 0.043(\text{Total P})$; 8; 0.27	Too few data
Cattle manure	$8.30 - 20.6(\text{Total N}) + 16.2(\text{Total N})^2$; 4; 0.99	$373 + 0.008(\text{Total P})$; 11; 0.22	$10400(1 - e^{(-0.0001 \times \text{Total K})}$; 11; 0.07
Biosolids	$857 - 529(\text{Total N}) + 127(\text{Total N})^2$; 24; 0.36	$e^{(0.0002 \times \text{Total P})}$; 11; 0.28	$232 + 0.048(\text{Total K})$; 17; 0.21

N, 2.2% of the total P, and 17% of the total K present. The authors also showed that softwoods could supply 27% and 6% of the total P and K present, respectively. Others have shown increases in available N, P, and K with softwood-based biochars (Dieguez-Alonso et al. 2018). Based on the current dataset, if producing biochars from hardwoods, K availability can be predicted relatively well based on total content ($R^2 = 0.87$) as compared to N and P. If, however, one produces biochars from softwoods, the availability of both N and K may be predicted relatively well based on total content ($R^2 = 0.68$ and 0.54, respectively).

In Sect. 6.1 above, it was stated that based on targeted biochar application rates of 0.5% to 1% (by wt.), one might need to apply at least 2000 mg of available N kg^{-1} to meet some of the major crop N demands (e.g., corn). Based on the predicted softwood N availability function (Table 6), it would require softwood total N contents to be ~7%. None of the softwood biochar data collected exceeded 4.5% (Figure S5A), and thus supplemental N fertilizers would be needed when utilizing softwood biochars applied to high N-demanding crops such as corn. Softwood biochars could likely be co-composted in order to capture available N, as described in Sect. 6.1 above. In addition, less N-demanding crops could potentially have N supplied by softwood biochars applied at reasonable application rates (i.e., 0.5–1% by wt.).

Applying K fertilizers to meet crop demands depends on soil K availability. Potassium applications could be as low as –56 kg K ha^{-1} (corn; Davis and Westfall 2014a) to as high as 250 kg ha^{-1} (corn or alfalfa; University of Delaware 2019; Lissbrant et al. 2009). We can predict soil K availability well with both hardwood ($R^2 = 0.87$) and softwood ($R^2 = 0.54$) biochars, with wood-based biochars averaging 1660 mg K kg^{-1} (Table 4). Using 1660 mg K kg^{-1} as a starting point, a biochar application rate of between 0.8 and 7% (by wt.) would be required to meet the aforementioned low- and high-end crop K demands. However, available K in hardwoods and softwoods can range from 0 up to either 13,000 or 4000 mg kg^{-1}, respectively (Figure S5G). At

almost 4–10 times greater than the average K concentration in wood-based biochars, application rates could easily be 4–10 times lower than the estimated 0.8–7% by wt. biochar application rates needed to meet crop K demands. Utilizing total K content in wood-based biochars could be used as a decision-making tool for K application and could specifically make hardwood and softwood biochar land applications attractive for supplying crop K demands globally.

6.5.2 Crop waste feedstocks

The use of agricultural crop waste products for biochar creation has occurred extensively throughout the world. The dataset created for the current study was dominated by a variety of crops, with the three major crops globally grown (i.e., corn, wheat, rice) utilized for predicting N, P, and K availability. One could potentially predict P availability marginally- to-well when utilizing any one of these three biochars (R^2 ranged from 0.48 to 0.82). Utilizing wheat straw biochars as a K source could be predicted fairly well based on total K present ($R^2 = 0.66$), while estimating N availability from these three crop-waste biochars appears to be weak at best ($R^2 = 0.02$–0.41).

As with any fertilizer, applying P fertilizers to meet crop demands is dependent on soil P availability. Phosphorus applications could be as low as 9 kg P ha^{-1} (band application to winter wheat; Davis and Westfall 2014b) to as high as 130 kg P ha^{-1} (broadcast application to corn; University of Delaware 2019). We can predict P availability fairly well with corn, wheat, or rice-based biochars, with crop waste averaging ~520 mg P kg^{-1} (Table 4). Using 520 mg P kg^{-1} as a starting point, a biochar application rate of between 0.8% and 11% (by wt.) would be required to meet the aforementioned low- and high-end crop P demands. Even though the available P in these three crop wastes ranges from 0 to 1800 mg kg^{-1} (Figure S5E), biochar applications to supply

crop P needs would likely only be warranted for those crops with low P requirements.

We can, however, predict wheat straw K availability fairly well. Wheat straw available K concentrations ranged from ~ 6000 to 30,000 mg kg^{-1} (Figure S5H), which were greater than those for hardwoods/softwoods. These results should make applying wheat straw-based biochars attractive for supplying most crop K demands globally and may solve a problem related to waste use in certain areas of the globe.

6.5.3 Manures/biosolids feedstocks

The use of manures or biosolids feedstocks for biochar creation has also been extensively studied globally. This may be driven by the fact that these feedstocks typically contain greater nutrient contents as compared to other feedstocks (e.g., Williams et al. 2017), and that pyrolyzing these materials represents a sound form of hygienization. Biochars made from these feedstocks have been shown to release available N (Liu et al. 2014; Sigua et al. 2016) in contrast to woody biochars. In the current study, N availability based on total biochar N content was predicted very well when utilizing either pig or cattle manure ($R^2 = 0.99$ and 0.99, respectively), but not with poultry or biosolids biochars. This suggests to biochar producers that, if they wanted to create a biochar that would act as an N fertilizer, that they either have to blend it with organic N-rich fertilizer materials (e.g. liquid manures, biogas digestate, vinasse, etc.) and use it as a carrier in low doses in the root zone (Schmidt et al. 2017) where 0.8–2 Mg ha^{-1} may suffice, or utilize either pig or cattle manure as a feedstock which might be also promising. As outlined in Sect. 6.1 above, based on a somewhat realistic biochar application rate (0.5–1.0% by wt.), one might need to apply at least 2000 mg of available N kg^{-1} to meet some of the major crop N demands (e.g., corn). Based on the predictive N functions in Table 6, pig or cattle manure would need to contain 3.8% or 11.7% total N, respectively. This total N content may be potentially feasible in pig manure (Figure S5C) if the material were sufficiently dried to concentrate total N (swine manures typically have low dry matter contents of 15–20%; e.g., McFarland et al. 2012). However, reaching 11.7% total N in cattle manure is likely nearly impossible given total N content ranges in the material and the relatively high dry matter content present (50–80%, e.g., McFarland et al. 2012). This leaves pig manure as the only biochar feedstock in the current study to have the potential to sufficiently supply N for crop growth without mixing the biochar with organic fertilizer materials, or use it in their treatment (e.g. composting; see: Godlewska et al. 2017; meta-study: Zhao et al. 2020).

It may be somewhat surprising that the prediction of available N from poultry manure and biosolids biochars was relatively low given that these feedstocks may contain greater initial N contents as compared to other biochar feedstocks (Figure S5C). However, the lack of prediction may simply be due to pyrolysis itself. Clough et al. (2013) noted that manures and biosolids pyrolysis can result in increasing aromatic and heterocyclic N structures within biochars, which are more difficult to degrade (i.e., recalcitrant).

It is also surprising to note that predicting either P or K availability was, at best, marginal with manures or biosolids-based biochars. Again, this may simply be due to pyrolysis itself. Biochars derived from manures and biosolids contain greater ash content (Table 1). As previously mentioned, this ash contains oxides, hydroxides, carbonates, as well as silicate phases (Novak et al. 2019a), that can form recalcitrant associations with K. Manure and biosolids derived biochars also contain greater Ca concentrations as compared to other biochars (Table 1), which, in combination with elevated alkalinity, pH, and aromatic C has been shown to reduce P solubility (Ngatia et al. 2017). This may also be the reason for lack of P fit for other biochars above (Wang et al. 2013).

Finally, the information presented above may lend itself for creating biochars from a combined variety of feedstocks. For example, mixing pig manure with agricultural crop wastes and hardwood or softwood, then pyrolyzing the combined materials, might effectively supply N, P, and K, respectively. Other researchers have followed a similar approach, albeit post biochar creation. Novak et al. (2014) blended manure biochar containing excessive P, with a nutrient poor biochar to achieve an end-product with a more balanced nutrient content. Sigua et al. (2016) utilized a 50:50 mix of softwood biochar with poultry manure biochar, observing a 670% and 830% increase in soil P and K, respectively. The promise of mixing feedstocks for balancing nutrient availability in biochars could be potentially realized based on the data presented in the current manuscript.

7 Conclusions

Understanding the influences that pyrolysis type, pyrolysis temperature, and initial feedstocks have on final biochar properties can help researchers and practitioners create biochars to meet agricultural environmental demands. Based on ~ 5400 published articles and over 50,000 individual observations, this project makes inferences to further our understanding of biochar physicochemical properties from the broad to specific and minute perspective. As compared to fast pyrolysis, slow pyrolysis leads to biochars containing greater SSA, CCE, ash content, available Fe and NO$_3$ concentrations.

Pyrolysis temperature influences biochar stability, with temperatures > 500 °C generally leading to longer-term half-lives (> 1000 years). This, in combination with greater pyrolysis temperatures promoting more stable C structures,

greater SSA, and potential improvements in soil aeration, percolation, infiltration, and overall structure, potentially suggests that greater pyrolysis temperatures may lead to long-term soil improvements and C storage.

Perhaps the most important influence on final biochar properties is feedstock choice. Wood-based feedstocks typically led to biochars containing the greatest SSA as compared to other feedstocks; this, in combination with pyrolysis temperature could greatly influence soil improvements. Crop-, grass-, and manures/biosolids-based feedstocks led to biochars containing elevated CECs as compared to wood-based biochars, which could affect nutrient sorption following land application. Based on the complete dataset collected, it appears possible to predict some plant-available biochar nutrients simply from total nutrient analysis. The collected data showed that we could reasonably predict (1) available N from softwood, corn, pig manure, and cattle manure biochars; (2) available P from corn, wheat, and rice straw/husk biochars; and (3) available K from hardwood, softwood, and wheat-derived biochars. This latter information could be useful when creating designer biochars for specific nutrient applications, simply by blending several feedstocks together. Based on this information, future research should test whether the available nutrient predictive functions, in combination with created mixed feedstock biochars, would hold true when placed within nutrient-poor soils.

References

Ahmad M, Lee SS, Dou XM, Mohan D, Sung JK, Yang JE, Ok YS (2012) Effects of pyrolysis temperature on soybean stover- and peanut shell-derived biochar properties and TCE adsorption in water. Bioresour Technol 118:536–544

Ahmad M, Lee SS, Lim JE, Lee SE, Cho JS, Moon DH, Hashimoto Y, Ok YS (2014) Speciation and phytoavailability of lead and antimony in a small arms range soil amended with mussel shell, cow bone and biochar: EXAFS spectroscopy and chemical extractions. Chemosphere 95:433–441

Ajayi AE, Horn R (2016) Modification of chemical and hydrophysical properties of two texturally differentiated soils due to varying magnitudes of added biochar. Soil Till Res 164:34–44

Amoah-Antwi C, Kwiatkowska-Malina J, Thornton SF, Fenton O, Malina G, Szara E (2020) Restoration of soil quality using biochar and brown coal waste: a review. Sci Tot Environ 722:137852

Antal MJ, Grønli M (2003) The art, science, and technology of charcoal production. Ind Eng Chem Res 42:1619–1640

aqion (2019) pH of common acids and bases. https://www.aqion.de/site/191. Accessed 27 July 2020

Asadullah M, Zhang S, Li C-Z (2010) Evaluation of structural features of chars from pyrolysis of biomass of different particle sizes. Fuel Process Technol 91:877–881

Blum CS, Lehmann J, Solomon D, Caires EF, Alleoni LRF (2013) Sulfur forms in organic substrates affecting S mineralization in soil. Geoderma 200–201:156–164

Bolan NS, Kunhikrishnan A, Choppala G, Thangarajan R, Chung J (2012) Stabilization of carbon in composts and biochars in relation to carbon sequestration and soil fertility. Sci Tot Environ 424:264–270

Borchard N, Siemens J, Ladd B, Möller A, Amelung W (2014) Application of biochars to sandy and silty soil failed to increase maize yield under common agricultural practice. Soil Till Res 144:184–194

Borchard N, Schirrmann M, Cayuela M, Kammann C, Wrage-Mönnig N, Estavillo JM, Fuertes-Mendizabal T, Sigua G, Spokas K, Ippolito JA, Novak J (2018) Biochar, soil and land use interactions that reduce nitrate leaching and N_2O emissions: a meta-analysis. Sci Tot Environ 651:2354–2364

Brewer CE, Hu Y-Y, Schmidt-Rohr K, Loynachan TE, Laird DA, Brown RC (2012) Extent of pyrolysis impacts on fast pyrolysis biochar properties. J Environ Qual 41:1115–1122

Briggs C, Breiner JM, Graham RC (2012) Physical and chemical properties of Pinus ponderosa charcoal: implications for soil modification. Soil Sci 177:263–268

Cantrell KB, Martin JH (2012) Stochastic state-space temperature regulation of biochar production. Part II: application to manure processing via pyrolysis. J Sci Food Agric 92:490–495

Cantrell KB, Hunt PG, Uchimiya M, Novak JM, Ro KS (2012) Impact of pyrolysis temperature and manure source on physicochemical characteristics of biochar. Bioresource Technol 107:419–428

Cao X, Harris W (2010) Properties of dairy-manure-derived biochar pertinent to its potential use in remediation. Bioresour Technol 101:5222–5228

Cao XF, Sun SN, Sun RC (2017) Application of biochar-based catalysts in biomass upgrading: a review. RCS Adv 7:48793–48805

Carpenter DL, Bain RL, Davis RE, Dutta A, Feik CJ, Gaston KR, Jablonski W, Phillips SD, Nimlos MR (2010) Pilot-scale gasification of corn stover, switchgrass, wheat straw, and wood: 1. Parametric study and comparison with literature. J Ind Eng Chem Res 49:1859–1871

Cayuela ML, Jeffery S, van Zwieten L (2015) The molar H: corg ratio of biochar is a key factor in mitigating N_2O emissions from soil. Agric Ecosyst Environ 202:135–138

Cha JS, Park SH, Jung SC, Ryu C, Jeon JK, Shin MC, Park YK (2016) Production and utilization of biochar: a review. J Indust Engineer Chem Res 40:1–15

Chang Y-M, Tsai W-T, Li M-H (2015) Chemical characterization of char derived from slow pyrolysis of microalgal residue. J Anal Appl Pyrol 111:88–93

Cheah S, Malone SC, Feik CJ (2014) Speciation of sulfur in biochar produced from pyrolysis and gasification of oak and corn stover. Environ Sci Technol 48:8474–8480

Chen B, Zhou D, Zhu L (2008) Transitional adsorption and partition of nonpolar and polar aromatic contaminants by biochars of pine needles with different pyrolytic temperatures. Environ Sci Technol 42:5137–5143

Chen H, Lin G, Wang X, Chen Y, Liu Y, Yang H, Shao J (2016) Physicochemical properties and hygroscopicity of tobacco stem biochar pyrolyzed at different temperatures. J Renew Sustain Energy 8:013112

Clough TJ, Condron LM, Kammann C, Müller C (2013) A review of biochar and soil nitrogen dynamics. Agronomy 3:275–293

Cui L, Yin C, Chen T, Quan J, Ippolito JA, Gan H, Xiao B, Pan M, Lui B, Yan J, Ding C, Hussain Q, Umer M (2019) Remediation of organic halogen- contaminated wetland soil using biochar. Sci Tot Environ 696:134087

Davis JG, Westfall DG (2014a) Fertilizing corn. Colorado State Extension Factsheet 0.538. https://extension.colostate.edu/topic-areas/agriculture/fertilizing-corn-0-538/. Accessed 27 July 2020

Davis JG, Westfall DG (2014b) Fertilizing winter wheat. Colorado State Extension Factsheet 0.544. https://extension.colostate.edu/topic-areas/agriculture/fertilizing-winter-wheat-0-544/. Accessed 27 July 2020

de Mendonça FG, da Cunha IT, Soares RR, Tristão JC, Lago RM (2017) Tuning the surface properties of biochar by thermal treatment. Bioresour Technol 246:28–33

Dieguez-Alonso A, Funke A, Anca-Couce A, Rombolà AG, Ojeda G, Bachmann J, Behrendt F (2018) Towards biochar and hydrochar engineering—influence of process conditions on surface physical and chemical properties, thermal stability, nutrient availability, toxicity and wettability. Energies 11:496

Domingues RR, Trugilho PF, Silva CA, de Melo ICNA, Melo LCA, Magriotis ZM, Sánchez-Monedero MA (2017) Properties of biochar derived from wood and high-nutrient biomasses with the aim of agronomic and environmental benefits. PLoS One 12:e0176884

Downie A, Crosky A, Munroe P (2009) Physical properties of biochar. In: Lehmann J, Joseph S (eds) Biochar for environmental management: science, technology and implementation, 1st edn. Routledge, New York, pp 227–249

Fuertes-Mendizábal T, Huérfano X, Vega-Mas I, Torralbo F, Menéndez S, Ippolito JA, Kammann C, Wrage-Mönnig N, Cayuela ML, Borchard N, Spokas K, Novak J, González-Moro MB, González-Murua C, Estavillo JM (2019) Biochar reduces the efficiency of nitrification inhibitor 3,4-dimethypyrazole phosphate (DMPP) mitigating N_2O emissions. Sci Reports. https://www.nature.com/articles/s41598-019-38697-2.pdf. Accessed 27 July 2020

Funke A, Ziegler F (2010) Hydrothermal carbonization of biomass: a summary and discussion of chemical mechanisms for process engineering. Biofuels Bioprod Biorefin 4:160–177

Godlewska P, Schmidt HP, Ok YS, Oleszczuk P (2017) Biochar for composting improvement and contaminants reduction. A review. Bioresour Technol 246:193–202

Gondek K, Mierzwa-Hersztek M (2016) Effect of low-temperature biochar derived from pig manure and poultry litter on mobile and organic matter-bound forms of Cu, Cd, Pb and Zn in sandy soil. Soil Use Manage 32:357–367

Guo J, Chen B (2014) Insights on the molecular mechanism for the recalcitrance of biochars: interactive effects of carbon and silicon components. Environ Sci Technol 48:9103–9112

Guo J, Lua AC (1998) Characterization of chars pyrolyzed from oil palm stones for the preparation of activated carbons. J Anal Appl Pyrol 46:113–125

Hagemann N, Joseph S, Schmidt H-P, Kammann CI, Harter J, Borch T, Young RB, Varga K, Taherymoosavi S, Elliott KW, McKenna A, Albu M, Mayrhofer C, Obst M, Conte P, Dieguez-Alonso A, Orsetti S, Subdiaga E, Behrens S, Kappler A (2017a) Organic coating on biochar explains its nutrient retention and stimulation of soil fertility. Nat Commun 8:1089

Hagemann N, Kammann CI, Schmidt H-P, Kappler A, Behrens S (2017b) Nitrate capture and slow release in biochar amended compost and soil. PLoS One 12:e0171214

Haider G, Steffens D, Müller C, Kammann CI (2016) Standard extraction methods may underestimate nitrate stocks captured by field aged biochar. J Environ Qual 45:1196–1204

Haider G, Steffens D, Moser G, Müller C, Kammann CI (2017) Biochar reduced nitrate leaching and improved soil moisture content without yield improvements in a four-year field study. Agric Ecosyst Environ 237:80–94

Hass A, Gonzalaz JM, Lima JM, Godwin HW, Halvorson JJ, Boyer DG (2012) Chicken manure biochar as liming and nutrient source for acid Appalachian soil. J Environ Qual 41:1096–1106

International Biochar Initiative (IBI) (2015) Standardized product definition and product testing guidelines for biochar that is used in soil. https://biochar-international.org/wp-content/uploads/2020/06/IBI_Biochar_Standards_V2.1_Final2.pdf. Accessed 27 July 2020

Ippolito JA, Strawn DG, Scheckel KG, Novak JM, Ahmedna M, Niandou MAS (2012) Macroscopic and Molecular Investigations of Copper Sorption by a Steam-Activated Biochar. J Environ Qual 41:1150–1156

Ippolito JA, Spokas KA, Novak JM, Lentz RD, Cantrell KB (2015) Biochar elemental composition and factors influencing nutrient retention. In: Lehmann J, Joseph S (eds) Biochar for environmental management: science, technology and implementation, 2nd edn. Routledge, New York, pp 137–161

Ippolito JA, Berry CM, Strawn DG, Novak JM, Levine J, Harley A (2017) Biochars reduce mine land soil bioavailable metals. J Environ Qual 46:411–419

Jeffery S, Verheijen FGA, Kammann C, Abalos D (2016) Biochar effects on methane emissions from soils: a meta-analysis. Soil Biol Biochem 101:251–258

Joseph S, Kammann CI, Shepherd JG, Conte P, Schmidt H-P, Hagemann N, Rich AM, Marjo CE, Allen J, Munroe P, Mitchell DRG, Donne S, Spokas K, Graber ER (2017) Microstructural and associated chemical changes during the composting of a high temperature biochar: mechanisms for nitrate, phosphate and other nutrient retention and release. Sci Total Environ 618:1210–1223

Kammann C, Linsel S, Gößling J, Koyro H-W (2011) Influence of biochar on drought tolerance of *Chenopodium quinoa* Willd and on soil–plant relations. Plant Soil 345:195–210

Kammann CI, Schmidt H-P, Messerschmidt N, Linsel S, Steffens D, Müller C, Koyro H-W, Conte P, Joseph S (2015) Plant growth improvement mediated by nitrate capture in co-composted biochar. Sci Reports 5:11080

Kim KH, Kim J-Y, Cho T-S, Choi JW (2012) Influence of pyrolysis temperature on physicochemical properties of biochar obtained from the fast pyrolysis of pitch pine (*Pinus rigida*). Bioresour Technol 118:158–162

Kinney TJ, Masiello CA, Dugan B, Hockaday WC, Dean MR, Zygourakis K, Barnes RT (2012) Hydrologic properties of biochars produced at different temperatures. Biomass Bioenergy 41:34–43

Kloss S, Zehetner F, Dellantonio A, Hamid R, Ottner F, Liedtke V, Schwanninger M, Gerzabek MH, Soja G (2012) Characterization of slow pyrolysis biochars: effects of feedstocks and pyrolysis temperature on biochar properties. J Environ Qual 41:990–1000

Knicker H (2007) How does fire affect the nature and stability of soil organic nitrogen and carbon? A review. Biogeochem 85:91–118

Knudsen JN, Jensen PA, Dam-Johansen K (2004) Transformation and release to the gas phase of Cl, K, and S during combustion of annual biomass. Energy Fuels 18:1385–1399

Kuzyakov Y, Bogomolova I, Glaser B (2014) Biochar stability in soil: decomposition during eight years and transformation as assessed by compound-specific ^{14}C analysis. Soil Biology Biochem 70:229–236

Laird DA, Novak JM, Collins HP, Ippolito JA, Karlen DL, Lentz RD, Sistani KR, Spokas K, Van Pelt RS (2017) Multi-year and multi-location soil quality and crop biomass yield responses to hardwood fast pyrolysis biochar. Geoderma 289:46–53

Lehmann J (2007) Bio-energy in the black. Fronti Ecol Environ 5:381–387

Lehmann J, Joseph S (2009) Biochar for environmental management: an introduction. In: Lehmann J, Joseph S (eds) Biochar for environmental management: science, technology and implementation, 1st edn. Routledge, New York, pp 1–12

Lehmann J, Pereira da Silva J, Steiner C, Nehls T, Zech W, Glaser B (2003) Nutrient availability and leaching in an archaeological Anthrosol and a Ferralsol of the Central Amazon basin: fertilizer, manure and charcoal amendments. Plant Soil 249:343–357

Lehmann J, Rillig MC, Thies J, Masiello CA, Hockaday WC, Crowley D (2011) Biochar effects on soil biota—a review. Soil Biology Biochem 43:1812–1836

Lentz RD, Ippolito JA (2012) Biochar and manure affect calcareous soil and corn silage nutrient concentrations and uptake. J Environ Qual 41:1033–1043

Lentz RD, Ippolito JA, Lehrsch GA (2019) Biochar, manure, and sawdust alter long-term water retention dynamics in degraded soil. Soil Sci Soc Am J 83:1491–1501

Lian F, Huang F, Chen W, Xing B, Zhu L (2011) Sorption of apolar and polar organic contaminants by waste tire rubber and its chars in single-and bi-solute systems. Environ Pollut 159:850–857

Liang B, Lehmann J, Solomon D, Kinyangi J, Grossman J, O'neill B, Skjemstad J, Thies J, Luizao F, Petersen J (2006) Black carbon increases cation exchange capacity in soils. Soil Sci Soc Am J 70:1719–1730

Lin Q, Xu X, Wang L, Chen Q, Fang J, Shen X, Lou L, Tian G (2017) The speciation, leachability and bioaccessibility of Cu and Zn in animal manure-derived biochar: effect of feedstock and pyrolysis temperature. Front Environ Sci Eng 11:5

Lissbrant S, Berg WK, Volanec J, Brouder S, Joern B, Cunningham S, Johnson K (2009) Phosphorus and potassium fertilization of alfalfa. Purdue University Extension Bulletin AY-331-W

Liu X, Zhang A, Ji C, Joseph S, Bian R, Li L, Pan G, Paz-Ferreiro J (2013) Biochar's effect on crop productivity and the dependence on experimental conditions-a meta-analysis of literature data. Plant Soil 373:583–594

Liu Y, Liu Y, Ding Y, Zheng J, Zhou T, Pan G, Crowley D, Li L, Zheng J, Zhang X, Yu X, Wang J (2014) Abundance, composition and activity of ammonia oxidizer and denitrifier communities in metal polluted rice paddies from south China. PLoS One 9:e102000

Lu J, Li J, Li Y, Chen B, Bao Z (2012) Use of rice straw biochar simultaneously as the sustained release carrier of herbicides and soil amendment for their reduced leaching. J Agric Food Chem 60:6463–6470

Luo L, Xu C, Chen Z, Zhang S (2015) Properties of biomass-derived biochars: combined effects of operating conditions and biomass types. Bioresour Technol 192:83–89

McFarland ML, Provin TL, Feagley SE (2012) Managing crop nutrients through soil, manure and effluent testing. Texas A&M AgriLife Extension Bulletin E-536

Nelissen V, Rütting T, Huygens D, Staelens J, Ruysschaert G, Boeckx P (2012) Maize biochars accelerate short-term soil nitrogen dynamics in a loamy sand soil. Soil Biology Biochem 55:20–27

Ngatia L, Hsieh Y, Nemours D, Fu R, Taylor R (2017) Potential phosphorus eutrophication mitigation strategy: biochar carbon composition, thermal stability and pH influence phosphorus sorption. Chemosphere 180:201–211

Nguyen TTN, Xu CY, Tahmasbian I, Che RX, Xu ZH, Zhou XH, Wallace HM, Bai SH (2017) Effects of biochar on soil available inorganic nitrogen: a review and meta-analysis. Geoderma 288:79–96

Novak JM, Lima I, Xing B, Gaskin JW, Steiner C, Das KC, Ahmedna M, Rehrah D, Watts DW, Busscher WJ, Schomberg H (2009) Characterization of designer biochar produced at different temperatures and their effects on a loamy sand. Ann Environ Sci 3:195–206

Novak JM, Cantrell KB, Watts DW, Busscher WJ, Johnson MG (2014) Designing relevant biochars as soil amendments using lignocellulosic-based and manure-based feedstocks. J Soils Sediments 14:330–343

Novak JM, Ippolito JA, Lentz RD, Spokas KA, Bolster CH, Sistani K, Trippe KM, Johnson MG (2016) Soil health, crop productivity, microbial transport, and mine spoil response to biochars. Bioenergy Res 9:454–464

Novak J, Ippolito JA, Watts DW, Sigua GC, Ducey TF, Johnson MG (2019a) Biochar compost blends facilitates switchgrass growth in mine soils by reducing Cd and Zn bioavailability. Biochar 1:97–114

Novak JM, Sigua GC, Ducey TF, Watts DW, Stone KC (2019b) Designer biochars impact on corn grain yields, biomass production, and fertility properties of a highly-weathered Ultisol. Environments 6:64

Pariyar P, Kumari K, Jain MK, Jadhao PS (2020) Evaluation of change in biochar properties derived from different feedstock and pyrolysis temperature for environmental and agricultural application. Sci Total Environ 713:136433

Qambrani NA, Rahman MM, Won S, Shim S, Ra C (2017) Biochar properties and eco-friendly applications for climate change mitigation, waste management, and wastewater treatment: a review. Renew Sustain Energy Rev 79:255–273

Sager M (2012) Levels of sulfur as an essential nutrient element in the soil-crop-foods system in Austria. Agriculture 2:1–11

Schimmelpfennig S, Glaser B (2012) One step forward toward characterization: some important material properties to distinguish biochars. J Environ Qual 41:1001–1013

Schmidt H-P, Pandit BH, Cornelissen G, Kammann C (2017) Biochar-based fertilization with liquid nutrient enrichment: 21 field trials covering 13 crop species in Nepal. Land Degrad Dev 28:2324–2342

Schmidt H-P, Anca-Couce A, Hagemann N, Werner C, Gerten D, Lucht W, Kammann C (2019) Pyrogenic carbon capture & storage (PyCCS). GCB Bioenergy 11:573–591

Sigua GC, Novak JM, Watts DW (2016) Ameliorating soil chemical properties of a hard setting subsoil layer in Coastal Plain USA with different designer biochars. Chemosphere 142:168–175

Sigua GC, Novak JM, Watts DW, Ippolito JA, Ducey TF, Johnson MG, Spokas KA (2019) Phytostabilization of Zn and Cd in mine soil using corn in combination with manure-based biochar and compost. Environments 6:69

Sistani KR, Novak JM (2006) Trace metal accumulation, movement and remediation in soils receiving animal manure. In: Prasad MN, Sajwan KS, Naidu R (eds) Trace elements in the environment, biogeochemistry, biotechnology, and bioremediation. CRC Press, Boca Raton, pp 689–706

Smith P, Adams J, Beerling DJ, Beringer T, Calvin KV, Fuss S, Griscom B, Hagemann N, Kammann C, Kraxner F, Minx JC, Popp A, Renforth P, Vicente JLV, Keesstra S (2019) Impacts of land-based greenhouse gas removal options on ecosystem services and the United Nations Sustainable Development Goals. Annu Rev Environ Resour 44:255–286

Sohi S, Lopez-Capel E, Krull E, Bol R (2009) Biochar, climate change and soil: a review to guide future research. CSIRO Land Water Sci Rep 5:17–31

Spokas KA (2010) Review of the stability of biochar in soils: predictability of O: C molar ratios. Carbon Manag 1:289–303

Tripathi M, Sahu JN, Ganesan P (2016) Effect of process parameters on production of biochar from biomass waste through pyrolysis: a review. Renew Sustain Energy Rev 55:467–481

Tsai W-T, Liu S-C, Chen H-R, Chang Y-M, Tsai Y-L (2012) Textural and chemical properties of swine-manure-derived biochar pertinent to its potential use as a soil amendment. Chemosphere 89:198–203

University of Delaware, College of Agriculture and Natural Resources Soil Testing Program (2019) Grain corn. https://www.udel.edu/content/dam/udelImages/canr/pdfs/extension/factsheets/AGR-Grain-Corn.pdf. Accessed 27 July 2020

Wang Y, Hu Y, Zhao X, Wang S, Xing G (2013) Comparisons of biochar properties from wood material and crop residues at different temperatures and residence times. Energy Fuels 27:5890–5899

Wang J, Xiong Z, Kuzyakov Y (2016) Biochar stability in soil: meta-analysis of decomposition and priming effects. Global Change Biol Bioenergy 8:512–523

Weber K, Quicker P (2018) Properties of biochar. Fuel 217:240–261

Werner C, Schmidt H-P, Gerten D, Lucht W, Kammann C (2018) Biogeochemical potential of biomass pyrolysis systems for limiting global warming to 1.5°C. Environ Res Lett 13:044036

Williams CL, Westover TL, Emerson RM, Tumuluru JS, Li C (2016) Sources of biomass feedstock variability and the potential impact on biofuels production. Bioenergy Res 9:1–14

Williams CL, Emerson RM, Tumuluru JS (2017) Biomass compositional analysis for conversion to renewable fuels and chemicals. In: Tumuluru JS (ed) Biomasss volume estimation and valorization for energy. IntechOpen Limited, London. https://doi.org/10.5772/65777

Wolf M, Lehndorff E, Wiesenberg GLB, Stockhausen M, Schward L, Amelung W (2013) Towards reconstruction of past fire regimes from geochemical analysis of charcoal. Organic Geochem 55:11–21

Woolf D, Lehmann J, Cowie A, Cayuela ML, Whitman T, Sohi S (2018) Biochar for climate change mitigation. In: Lal R, Stewart BA (eds) Navigating from science to evidence-based policy. Advances in Soil Science, Soils and Climate. CRC Press. ISBN 9781498783651. http://www.css.cornell.edu/faculty/lehmann/publ/Woolf%20et%20al%202018%20Biochar%20for%20Climate%20Change%20Mitigation.pdf. Accessed 27 July 2020

Zhang H, Chen C, Gray EM, Boyd SE (2017a) Effect of feedstock and pyrolysis temperature on properties of biochar governing end use efficacy. Biomass Bioenergy 105:136–146

Zhang H, Voroney RP, Price GW (2017b) Effects of temperature and activation on biochar chemical properties and their impact on ammonium, nitrate, and phosphate Sorption. J Environ Qual 46:889–896

Zhao Y, Zhao L, Mei Y, Li F, Cao X (2018) Release of nutrients and heavy metals from biochar-amended soil under environmentally relevant conditions. Environ Sci Pollut Res 25:2517–2527

Zhao S, Schmidt S, Qin W, Li J, Li G, Zhang W (2020) Towards the circular nitrogen economy—a global meta-analysis of composting technologies reveals much potential for mitigating nitrogen losses. Sci Total Environ 704:135401

Affiliations

James A. Ippolito[1] · Liqiang Cui[1,2] · Claudia Kammann[3] · Nicole Wrage-Mönnig[4] · Jose M. Estavillo[5] · Teresa Fuertes-Mendizabal[5] · Maria Luz Cayuela[6] · Gilbert Sigua[7] · Jeff Novak[7] · Kurt Spokas[8] · Nils Borchard[9]

James A. Ippolito
Jim.Ippolito@colostate.edu

1. Department of Soil and Crop Sciences, Colorado State University, Fort Collins 80523, USA

2. School of Environmental Science and Engineering, Yancheng Institute of Technology, 9 Yingbin Avenue, Yancheng 224051, China

3. Department of Applied Ecology, Geisenheim University, Von-Lade-Straße 1, 65366 Geisenheim, Germany

4. Faculty of Agricultural and Environmental Sciences, Grassland and Fodder Sciences, University of Rostock, Justus-von-Liebig-Weg 6, 18059 Rostock, Germany

5. Department of Plant Biology and Ecology, University of the Basque Country (UPV/EHU), Apdo. 644, 48080 Bilbao, Spain

6. Department of Soil and Water Conservation and Waste Management, CEBAS-CSIC, Campus Universitario de Espinardo, 30100 Murcia, Spain

7. United States Department of Agriculture, Agriculture Research Service, Coastal Plains Research Center, 2611 West Lucas Street, Florence, SC 29501, USA

8. United States Department of Agriculture, Agriculture Research Service, Soil and Water Management Research Unit, University of Minnesota, 439 Borlaug Hall, 1991 Buford Circle, St. Paul, MN 29501, USA

9. Natural Resources Institute Finland (Luke), Latokartanonkaari 9, 00790 Helsinki, Finland